7 The role of wind tunnels

7.1 Introduction

Most practising structural engineers will not themselves operate wind tunnels, but they may be clients of wind tunnel groups who will provide wind loading information for new or existing structures, usually by means of model tests. For this reason, this chapter will not attempt to describe wind tunnel techniques in detail. There are detailed references, guide books and manuals of practice available which perform this function (e.g. Cermak, 1977; Reinhold, 1982; Australasian Wind Engineering Society, 2001; American Society of Civil Engineers, 1999). However sufficient detail is given here to enable the educated client to be able to 'ask the right questions' of their wind tunnel contractors.

In the following sections, a brief description of wind tunnel layouts is given, and methods of simulation of natural wind flow and experimental measurement techniques are discussed.

7.2 Wind tunnel layouts

7.2.1 Historical

The first use of a wind tunnel to measure wind forces on buildings is believed to have been made by Kernot in Melbourne, Australia (1893). A sketch of the apparatus, which he called a 'blowing machine', is given in Figure 7.1 (Aynsley *et al.*, 1977). This would now be described as an 'open-circuit, open test-section' arrangement. With this equipment, Kernot studied wind forces on a variety of bluff bodies – cubes, pyramids, cylinders, etc., and on roofs of various pitches.

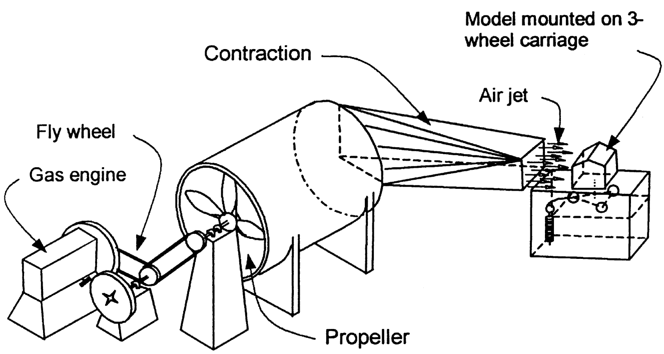

Figure 7.1 Sketch of W. C. Kernot's 'blowing machine' of 1893 (Aynsley *et al.*, 1977).

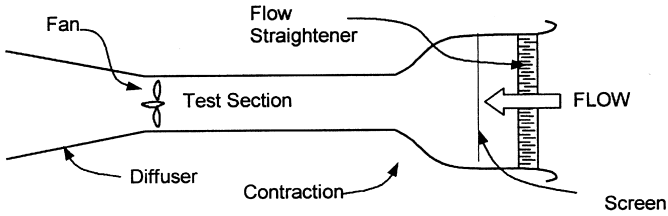

Figure 7.2 Layout of an open-circuit wind tunnel.

At about the same time, Irminger (1894) in Copenhagen, Denmark used the flow in a flue of a chimney to study wind pressures on some basic shapes (Larose and Franck, 1997).

Wind tunnels for aeronautical applications developed rapidly during the first half of the twentieth century, especially during and between the two world wars. The two basic wind tunnel layouts: the *open circuit*, or 'N.P.L. (National Physical Laboratory) type', and the *closed circuit*, or 'Göttingen-type' were developed during this period, named after the research establishments in the U.K. and Germany where they originated. These two types are outlined in the following sections.

7.2.2 Open-circuit type

The simplest type of wind tunnel layout is the open-circuit or N.P.L. type. The main components are shown in Figure 7.2. The contraction, usually with a flow straightener, and fine mesh screens, has the function of smoothing out mean flow variations, and reducing turbulence in the test section. For modelling atmospheric boundary layer flows, which are themselves very turbulent, as described in Chapter 3, it is not essential to include a contraction, although it is better to start with a reasonably uniform and smooth flow before commencing to simulate atmospheric profiles and turbulence.

The function of the diffuser, shown in Figure 7.2, is to conserve power by reducing the amount of kinetic energy that is lost with the discharging air. Again this is not an essential item, but omission will be at the cost of higher electricity charges.

Figure 7.2 shows an arrangement with an axial-flow fan downstream of the test section. This arrangement is conducive to better flow, but since the function of the fan is to produce a pressure rise to overcome the losses in the wind tunnel, there will be a pressure drop across the walls and floor of the test section that can be a problem if leaks exist. An alternative is a 'blowing' arrangement in which the test section is downstream of the fan (see Figure 7.5). Usually a centrifugal blower is used, and a contraction with screens is

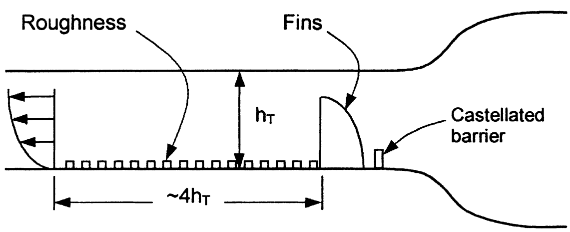

Figure 7.3 The Counihan method for short test sections.

essential to eliminate the swirl downstream of the fan. However, in this arrangement the test section is at or near atmospheric pressure.

Both the arrangements described above have been used successfully in wind engineering applications.

7.2.3 Closed-circuit type

In the closed circuit, or Göttingen-type, wind tunnel, the air is continually recirculated, instead of being expelled. The advantages of this arrangement are as follows:

- It is generally less noisy than the open-circuit type
- It is usually more efficient. Although the longer circuit gives higher frictional losses, there is no discharge of kinetic energy at exit
- More than one test section with different characteristics can be incorporated.

However, this type of wind tunnel has a higher capital cost, and the air heats up over a long period of operation before reaching a steady-state temperature. This can be a problem when operating temperature-sensitive instruments, such as hot-wire or other types of thermal anemometers, which use a cooling effect of the moving air for their operation.

7.3 Simulation of the natural wind flow

In this section, methods of simulation of strong wind characteristics in a wind tunnel are reviewed. Primarily, the simulation of the atmospheric boundary layer in gale, or large-scale synoptic conditions, is discussed. This type of large-scale storm is dominant in the temperate climates, for latitudes greater than about 40 degrees, as discussed in Chapter 1.

Even in large scale synoptic windstorms, flows over sufficiently long homogeneous fetch lengths, so that the boundary-layer is fully developed, are relatively uncommon. They will occur over open sea with consistent wave heights, and following large fetches of flat open country or desert terrain. Buildings or other structures, which are exposed to these conditions, are few in number, however. Urban sites, with flat homogeneous upwind roughness of sufficient length to produce full development of the boundary layer, are also relatively uncommon. However, there have been sufficient measurements in conditions that are close to ideal to produce generally accepted semi-theoretical models of the strong-wind atmospheric boundary layer for engineering purposes. These models have been validly used as the basis for wind tunnel modelling of phenomena in the atmosphere, and the salient points have been discussed in Chapter 3.

In the case of the wind loading and response of structures, such as buildings, towers, bridges, etc., gales produced by large, mature, extra-tropical, depressions are adequately described by these models, and they form a benchmark by which wind tunnel flows are usually assessed. However, there are significant differences of opinion regarding some turbulence properties, such as length scales and spectra, which are important in determining wind forces and dynamic response. These uncertainties should be considered when assessing the reliability of wind tunnel tests as a predictor of wind effects on real structures.

As outlined in Chapter 3, these models are also not good ones for storm winds produced by localized thermal mechanisms, namely tropical cyclones (hurricanes, typhoons), thunderstorms (including tornadoes) and monsoons. Winds produced by these storms are the dominant ones for design of structures in latitudes within about 40 degrees from the Equator.

The following sections consider natural growth methods requiring long test sections, methods used for wind tunnels with short test sections, and methods developed for simulating only the inner or surface layer of the atmospheric boundary layer. Finally some possibilities for simulations of strong winds in tropical cyclone and thunderstorm conditions are discussed. Laboratory modelling of these phenomena is still in an early stage of development, but some ideas on the subject are presented in Section 7.3.4.

7.3.1 Similarity criteria and natural growth methods

The 'ideal' neutral atmospheric boundary layer has two characteristic length scales – one for the outer part of the flow which depends on the rate of rotation of the earth and the latitude and on a velocity scale, and one for the flow near the surface itself which depends on the size and density of the roughness on the surface. The region near the surface, which is regarded as being independent of the effects of the earth's rotation, has a depth of about 100 m, and is known as the *inner* or *surface layer*.

The first deliberate use of boundary-layer flow to study wind pressure on buildings was apparently by Flachsbart (1932). However, the work of Martin Jensen in Denmark provided the foundation for modern boundary-layer wind tunnel testing techniques. Jensen (1958) suggested the use of the inner layer length scale, or roughness length z_0 (see Section 3.2.1), as the important length scale in the atmospheric boundary-layer flow, so that for modelling phenomena in the natural wind, ratios such as building height to roughness length (h/z_0) – later known as the Jensen number, are important. Jensen (1965) later described model experiments carried out in a small wind tunnel in Copenhagen, in which natural boundary layers were allowed to grow over a fetch of uniform roughness on the floor of the wind tunnel. In the 1970s larger 'boundary-layer' wind tunnels were constructed, and began to be used for wind engineering studies of tall buildings, bridges and other large structures (Cermak, 1971; Davenport and Isyumov, 1967), These tunnels are either of closed circuit design (Section 7.2.3), or open circuit of the 'sucking' type, with the axial flow fan mounted downstream of the test section (Section 7.2.2). In more recent years, several open circuit wind tunnels of the 'blowing' type have been constructed with a centrifugal fan upstream of the test section, supplying it through a rapid diffuser, a settling chamber containing screens and a contraction. As discussed in Section 7.2.3, the latter system has the advantage of producing nearly zero static pressure difference across the wind tunnel walls at the end of the boundary-layer test section.

A naturally grown rough-wall boundary layer will continue to grow until it meets the boundary layer on the opposite wall or roof. In practical cases, this equilibrium situation is not usually reached, and tests of tall structures are carried out in boundary layers that are still developing, but are sufficient to envelop the model completely. In most cases of structural tests, more rapid boundary-layer growth must be promoted by a 'tripping' fence or grid at the start of the test section. Dimensional analysis indicates that the full height of the atmospheric boundary layer depends on the wind speed and the latitude. However, the typical height is about 1000 m. Assuming a geometric scaling ratio of 1/500, this means that a *minimum* wind tunnel height of 2 m is required to model the full atmospheric boundary layer. Usually a lower boundary layer height is accepted, but the turbulent boundary-layer flow should completely envelop any structure under test.

In the early days of boundary-layer wind tunnels, it was common to install a roof of adjustable height for the purpose of maintaining a constant pressure gradient in the along-wind direction. This allows for the increasing velocity deficit in the flow direction, and maintains the 'free-stream' velocity outside the boundary layer approximately constant.

This should also reduce the errors due to blockage for large models. For smaller models with lower blockage ratios, the errors in the measurements when the roof is maintained at a constant height, or with a fixed slope are quite small, and it has been found to be unnecessary to continually adjust the roof, in most situations. Blockage errors and corrections are discussed in Section 7.4.

As noted previously, the real atmospheric boundary layer is affected by the earth's rotation, and apparent forces of the Coriolis type must be included when considering the equations of motion of air flow in the atmosphere. One effect of this is to produce a mean velocity vector which is not constant in direction with height; it is parallel to the pressure gradient at the top of the boundary layer (or 'gradient' height), and rotates towards the lower static pressure side as the ground level is approached. This effect is known as the 'Ekman Spiral' (although the original solution by Ekman was obtained by assuming a shear stress in the flow proportional to the vertical velocity gradient – an assumption later shown to be unrealistic), and it has been shown to occur in full scale, with mean flow direction changes up to 30 degrees having been measured. This effect cannot be achieved in conventional wind tunnels, and the direction change is usually regarded as unimportant over the heights of most structures.

7.3.2 Methods for short test sections

In the 1960s and 1970s, to avoid the costs of constructing new boundary-layer wind tunnels, several methods of simulating the atmospheric boundary layer in existing (aeronautical) wind tunnels with test sections of low aspect ratio, i.e. short with respect to their height and width, were investigated. These usually make use of tapered fins or spires, which produce an immediate velocity gradient downstream, and which develops into a mean velocity profile representative of that in the atmosphere within a short downstream distance. Other bluff devices, such as grids or barriers, are required upstream, together with roughness on the floor of the wind tunnel, to increase the turbulence intensities to full-scale values.

Flows produced by these methods are likely to be still in a process of rapid development at the end of the short test section, and the interaction of the vortex structures produced in the wakes of the various devices, may well result in unwanted characteristics in the turbulence at the measurement position. Unless detailed fluctuating velocity measurements, including spatial correlations, are made, such characteristics may never be detected. Fortunately, wind pressures and forces on structures appear to be dependent mainly on single point statistics, such as turbulence intensities, and integral length scales in the along-wind direction, and not on the detailed eddy structures within the turbulence, in the approach flow.

Of the several methods developed in the late 1960s and early 1970s, that of Counihan (1969) is perhaps the best documented. The upstream devices consisted of a castellated fence, or barrier, several elliptical 'sharks-fins', and a short fetch of surface roughness (Figure 7.3). Detailed measurements of mean velocity and turbulence intensity profiles at various spanwise stations, and of cross-correlations and spectra were made.

7.3.3 Simulation of the surface layer

For simulation of wind forces and other wind effects on low-rise buildings, say less than 10 m in height, geometric scaling ratios of 1/400 result in extremely small models and do not allow any details on the building to be reproduced. The large differences in Reynolds

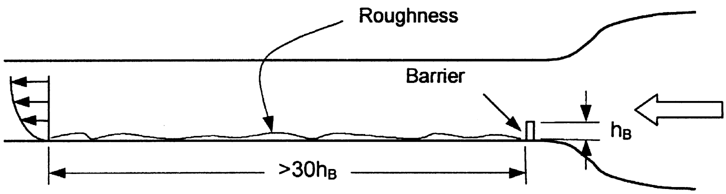

Figure 7.4 The barrier-roughness technique.

numbers between model and full scale may mean that the wind tunnel test data is quite unreliable. For this type of structure, no attempt should be made to model the complete atmospheric boundary layer. Simulation of the inner or surface layer, which is approximately 100 m thick in full scale, is sufficient for such tests. If this is done, larger and more practical scaling ratios in the range of 1/50 to 1/200 can be used for the models.

Cook (1973) developed a method for simulation of the lower third of the atmospheric boundary layer. This system consists of a castellated barrier, a mixing grid and surface roughness. A simpler system consisting of a plain barrier, or wall, at the start of the test section, followed by several metres of uniform surface roughness has also been used (Figure 7.4) (Holmes and Osonphasop, 1983). This system has the advantage that simultaneous control of the longitudinal turbulence intensity and the longitudinal length scale of turbulence, to match the model scaling ratio, is obtained by adjustment of the height of the barrier. Larger scales of turbulence can be produced by this method than by other approaches – large horizontal vortices with their axes normal to the flow are generated in the wake of the barrier. Studies of the development of the flow in the wake of the barrier (Holmes and Osonphasop, 1983) showed that a fetch length of at least 30 times the barrier height is required to obtain a stable and monotonically increasing mean velocity profile. However, there is still a residual peak in the shear stress profile at the height of the barrier at this downstream position; this shows that the flow is still developing at the measurement position, but the effect of this on pressures on and flow around single buildings should not be significant.

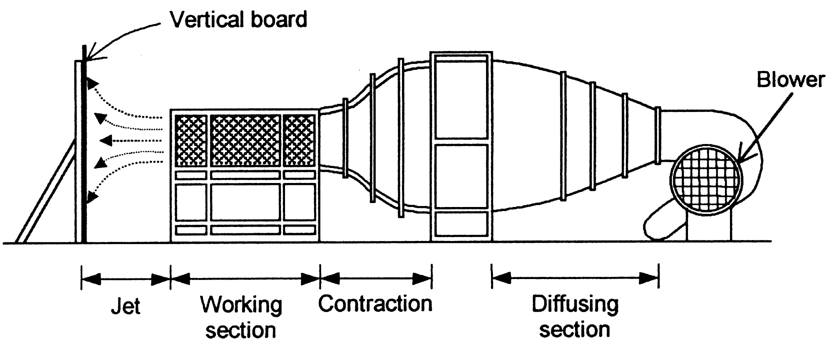

Figure 7.5 Simulation of thunderstorm downburst by impinging jet.

7.3.4 Simulation of tropical cyclone and thunderstorm winds

As discussed in Chapter 1, strong winds produced by tropical cyclones and thunderstorms dominate the populations of extreme winds in most locations with latitudes less than 40 degrees, including many sites in the U.S.A., Australia, India and South Africa. Unfortunately, full-scale measurements are few in number, and there are no available analytical models for the surface wind structures in these storms. However, the few full-scale measurements, and some meso-scale numerical models, have enabled qualitative characteristics of the winds to be determined.

Tropical cyclones, known also as 'hurricanes' and 'typhoons' in some parts of the world, are circulating systems with a complex three-dimensional wind structure near their centre (Section 1.3.2). At the outer radii, where the wind speeds are lower, a boundary-layer structure should exist and conventional boundary-layer wind tunnels should be quite adequate for flow modelling. However, the region of maximum horizontal winds occurs just outside the eye wall. Here the winds near the surface turn towards the low pressure centre, and in a spiralling upward direction at greater heights. Measurements have indicated a steeper mean velocity profile than would be expected for gales, for the surface roughness conditions around the site, up to height of about 100 m. Above that height, the mean wind velocity is approximately constant up to the top of the tower (Section 3.2.5). Measurements of turbulence intensities in typhoons have shown higher values than occur at the same site in non-cyclonic conditions (Section 3.3.1). As most structures do not exceed 100 m in height, a reasonable approximation to the tropical cyclone flow can be obtained by using a boundary-layer flow generated for urban terrain conditions, even for directions with lower roughness lengths, such as off-water winds for coastal sites.

The laboratory modelling of thunderstorm winds is a more difficult problem for a number of reasons. First there are a number of different types of local windstorms associated with thunderstorms, although some of these have similar characteristics. Second, these storms are individually transient, although a number of them may occur sequentially on the same day. The length of an individual storm rarely exceeds thirty minutes. Third, thunderstorm winds are driven by thermodynamic processes which probably cannot be reproduced in a laboratory simulation.

The velocity profile in a thunderstorm downdraft is quite similar to a wall jet. The latter has been proposed as a laboratory model of the flow in a downdraft, and some studies have been conducted using the outlet jet from a wind tunnel impinging on a vertical board, as shown in Figure 7.5. Measurements can be carried out at various radial positions from the centre of the board. This system gives velocity profiles which are quite similar to those measured by radar in microbursts, but the transient characteristics of the real downdraft flow are not reproduced, and the turbulence characteristics in the two flows could be quite different.

7.4 Modelling of structures for wind effects

The modelling of structures for wind effects requires knowledge of dimensional analysis and the theory of modelling (e.g. Whitbread, 1963).

The general approach is as follows. It may be postulated that the response of a structure to wind loading, including resonant dynamic response, is dependent on a number of basic variables, such as the following (not necessarily exclusive): $\bar{U}$, the mean wind speed at some reference position; z_0, roughness length defining the approaching terrain and velocity profile (Section 3.2.1); σ_u, standard deviation of longitudinal turbulence; σ_v, standard deviation of lateral turbulence; σ_w, standard deviation of vertical turbulence, ℓ_u, length scale of longitudinal turbulence (Section 3.3.4); ℓ_v, length scale of lateral turbulence; ℓ_w, length scale of vertical turbulence; ρ_a, density of air; ν, viscosity of air; g, acceleration due to gravity; ρ_s, density of the structure; E, Young's modulus for the structural material; G, Shear modulus for the structural material; η, structural damping ratio; L, characteristic length of the structure.

The above list has been simplified considerably. For example, for a bridge there will usually be different structural properties for the deck, the towers, the cables, etc. However, the above list will suffice to illustrate the principles of structural modelling.

The above sixteen dimensioned variables can be reduced to thirteen (16 – 3) independent dimensionless groups, according to the Buckingham-Pi theorem. A possible list of these is as follows: L/z_0, Jensen number; $\sigma_u/\bar{U}$, longitudinal turbulence intensity; $\sigma_v/\bar{U}$, lateral turbulence intensity; $\sigma_w/\bar{U}$, vertical turbulence intensity; ℓ_u/L, length ratio; ℓ_v/L, length ratio; ℓ_w/L, length ratio; $\frac{\bar{U}}{L\nu}$, Reynolds number (Section 4.2.4); ρ_s/ρ_a, density ratio; $\frac{\bar{U}}{\sqrt{Lg}}$, Froude number (inertial forces (air)/gravity forces (structure)); $\frac{E}{\rho_a\bar{U}^2}$, Cauchy number (normal internal forces in structure/inertial forces (air)); $\frac{G}{\rho_a\bar{U}^2}$, Cauchy number (internal shear forces in structure/inertial forces (air)); η, critical damping ratio.

For correct scaling, or similarity in behaviour between the model and full-scale structure, these non-dimensional groups should be numerically equal for the model (wind tunnel) and prototype situation.

The thirteen groups are not a unique set. Other non-dimensional groups can be formed from the sixteen basic variables, but there are only thirteen *independent* groups, and it will be found that the additional groups can be formed by taking products of the specified groups or their powers.

For example, it is often convenient to replace a Cauchy number by a reduced frequency (n_sL/U), where n_s is a structural frequency. For structures or structural members in bending, n_s is proportional to $\sqrt{(E/\rho_sL^2)}$.

Then the reduced frequency,

$$\frac{n_sL}{\bar{U}} = K\sqrt{\frac{E}{\rho_sL^2}}.\frac{L}{\bar{U}} = K\sqrt{\frac{E}{\rho_a\bar{U}^2}}.\sqrt{\frac{\rho_a}{\rho_s}} \tag{7.1}$$

where K is a constant.

Thus, the reduced frequency is proportional to the square root of the Cauchy number divided by the density ratio.

7.5 Measurement of local pressures

Modern cheap sensitive solid-state pressure sensors, either as individual transducers or as part of a multi-channel electronic scanning system, enable near-simultaneous measurements of fluctuating wind pressures on wind tunnel models of buildings and structures for up to several hundred measurement positions (Holmes, 1995).

For reasons of cost or geometric constraint, it is usually necessary to mount the pressure sensor or scanning unit remotely from the point where the pressure measurement is required. Then the fluctuating pressure must be transmitted by tubing between the measurement and sensing points. The dynamic frequency response of the complete pressure measurement system, including the sensor itself, the volume exposed to the diaphragm, and the tubing, is an important consideration.

Inadequate response can lead to significant errors especially when measuring peak pressures or suctions on building models (e.g. Durgin, 1982; Holmes, 1984; Irwin, 1988). As a rule of thumb, the equivalent full-scale upper frequency response limit should not be less than about 2 Hz. To convert this to model frequency, the frequency ratio is obtained by dividing the velocity ratio by the geometric length scaling ratio, e.g for a typical velocity ratio of 1/3, and a geometric ratio of 1/300, the frequency ratio is 100, and the desirable upper limit is 200 Hz.

The transmission of pressure fluctuations is affected by the mass inertia, compressibility, and energy dissipation in the transmitting fluid. Standing waves can produce unwanted resonant peaks in the amplitude frequency response characteristics of the system, and a nonlinear variation of phase lag with frequency (e.g. Bergh and Tijdeman, 1965).

An ideal system would have an amplitude response which is constant over the frequencies of interest, and a linear phase variation with frequency. The latter characteristic guarantees that there is no distortion of transient pressure 'signatures' by the system.

As well as pressure measurement at a single point, systems in which pressures from a number of points are connected to a common manifold or *pneumatic averager* have become widely used. In wind engineering, this arrangement has been used to obtain fluctuating and peak pressures appropriate to a finite area, or panel, on a building model in a turbulent wind tunnel flow (e.g. Surry and Stathopoulos, 1977; Holmes and Rains, 1981; Gumley, 1984; Holmes, 1987; Kareem *et al.,* 1989).

7.5.1 Single-point measurements

Three common systems are in use:

'Short' tube systems

This system uses a relatively short length of tubing to connect the measurement point to the sensor. Typically, for wind tunnel testing, this may consist of tubing 20–100 mm long, and 1–2 mm internal diameter. The short tube lengths will result in resonant frequencies that are high, hopefully well above the range of interest for the measurements. However, the short tube also results in low dissipation of energy, and the amplitude response rises to a high value at the peak.

'Restricted' tube systems

Restricted-tube systems may be defined as those involving one or more changes in internal diameter along the tube length. Such systems often allow location of pressure sensors at distances of 150–500 mm from the measurement point, with good amplitude and phase characteristics up to 200 Hz, or more. The simplest system of this type is the two-stage type, in which a section of narrower tube is inserted between the main tube section and the transducer. Restricted-tube systems are very effective in removing resonant peaks and giving linear phase response characteristics (e.g. Surry and Isyumov, 1977; Irwin *et al.*, 1979; Holmes and Lewis, 1987a). An effective frequency range can be obtained which is better than that for a constant diameter tubing with a fraction of the length.

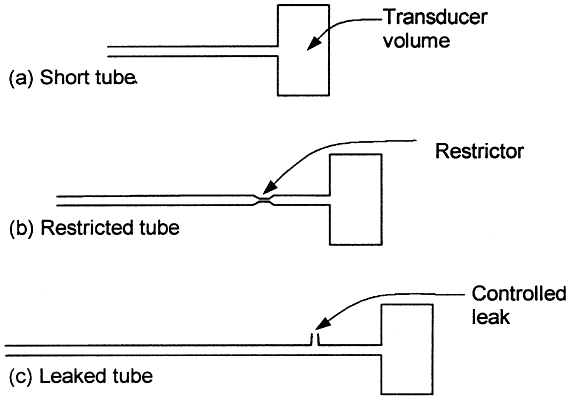

Figure 7.6 Tubing arrangements for measurement of point pressures.

'Leaked' tube systems

The leaked-tube system was proposed by Gerstoft and Hansen (1987). A theoretical model was developed by Holmes and Lewis (1989). A relatively flat amplitude frequency response to frequencies of 500 Hz, with 1 m of connecting tubing, is possible with a system of this type. This is achieved by inserting a controlled side leak part-way along the main connecting tube, usually close to the transducer. It has the effect of attenuating the amplitude response to low frequency fluctuations, and to steady pressures, to the level of a conventional closed system at higher frequencies. Thus, the leak effectively introduces a high-pass filter into the system. The amplitude ratio at frequencies approaching zero, is

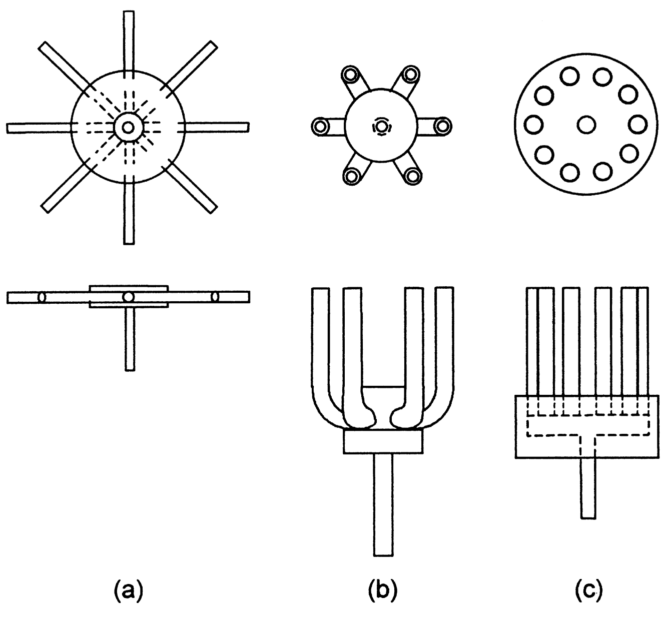

Figure 7.7 Manifolds for pressure averaging.

simply a function of the resistance to steady laminar flow of the main tube and leak tube. For multiple pressure tap measurements with this system, it is normally necessary to connect all the leaks to a common reference pressure, usually that inside a closed chamber, or plenum, to which the reference static pressure is also connected.

The general arrangement of the three types of single-point measurements are shown in Figure 7.6.

7.5.2 Measurement of area-averaged pressures

Systems which average the pressure fluctuations from a number of measurement points, so that area-averaged wind loads on finite areas of a structure can be obtained, are now in common use. Averaging manifolds were first used in wind tunnels by Surry and Stathopoulos (1977). Gumley (1981, 1983) developed a theoretical model for their response.

Figure 7.7 shows the types of parallel tube and manifold arrangement that have been commonly used in wind engineering work. Provided that the inlet tubes are identical in length and diameter, such a system should provide a true average in the manifold, of the fluctuating pressures at the entry to the input tubes, assuming that laminar flow exists in them. Usually, flatter amplitude response curves to higher frequencies, can be obtained with the multi-tube manifold systems, compared with single-point measurements using the same tube lengths, due to the reinforcement of the higher frequencies in the input tubes. However, once the number of input tubes exceeds about five, there is little change to the response characteristics. The response is also not greatly sensitive to the volume of the averaging manifold.

The assumption that the average of discrete fluctuating point pressures, sampled within a finite area of a surface, adequately approximates the continuous average aerodynamic load on the surface requires consideration (Surry and Stathopoulos, 1977; Holmes and Lewis, 1987b).

Figure 7.8 shows the ratio of the variance of the averaged panel force to the variance of the point pressure, using first, the correct continuous averaging over the panel denoted by R_c, and second, the discrete averaging approximation performed using the pneumatic averaging system with the ten pressure tappings within a panel, denoted by R_d. Calculations of these ratios were made, assuming a correlation coefficient for the fluctuating pressures

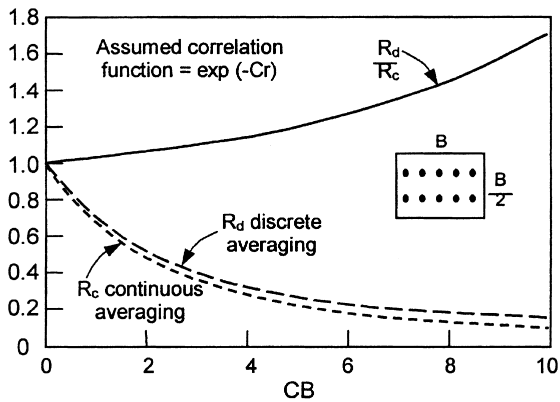

Figure 7.8 Discrete and continuous averaging of fluctuating pressures.

of the form, exp(−*Cr*), where *r* is a separation distance, and *C* is a constant. The variance of the local pressure fluctuations across the panel of dimensions *B* by *B*/2, were assumed constant.

It can be seen that R_d exceeds R_c for all values of *CB*. This is due to the implied assumption, in the discrete averaging, that the pressure fluctuations are fully correlated in the tributary area around each pressure tap. Clearly, the error increases with increasing *C* due to the lower correlation of the pressure fluctuations, and with increasing panel size, *B*. The errors can be decreased by increasing the number of pressure tappings within a panel of a certain size. However, it should be noted that the errors are larger at higher frequencies than at lower frequencies; a more detailed analysis of the errors requires knowledge of the coherence of the pressure fluctuations.

7.5.3 Equivalent time averaging

An alternative procedure for determining wind loads acting over finite surface areas from point pressures is known as 'equivalent time averaging'. In this approach, the time histories of fluctuating point pressures are filtered by means of a moving average filter. As originally proposed by Lawson (1976), the averaging time, τ, was estimated to be given by the following formula:

$$\tau \cong 4.5\frac{L}{\bar{U}} \qquad (7.2)$$

where *L* is usually taken as the length of the diagonal for the panel of interest.

However, a later analysis (Holmes, 1997) showed equation (7.2) to be unconservative, and that a more correct relationship is:

$$\tau \cong 1.0\frac{L}{\bar{U}} \qquad (7.3)$$

However the 'constants' in the above equations are likely to vary considerably depending on the location of the pressure measurement position on a building model – i.e. windward wall, roof, etc. This method is less accurate than the area-averaging technique by manifolding described in Section 7.5.2.

7.6 Modelling of overall loads and response of structures

7.6.1 Base-pivotted model testing of tall buildings

This section describes the procedure for the conducting of aeroelastic wind tunnel testing of high-rise buildings, using rigid models.

The use of rigid-body aeroelastic modelling of tall buildings is based on three basic assumptions:

- The resonant response of the building to wind loads in torsional (twisting modes) can be neglected
- The response in sway modes higher than the first in each orthogonal direction, can be neglected

- The mode shapes of the fundamental sway modes can be assumed to be linear.

With these assumptions, the motion of a rigid model of the building, pivotted at, or near, ground level, and located in a wind tunnel in which an acceptable model of the atmospheric boundary layer in strong winds has been set up, can be taken to represent the sway motion of the prototype building. The fact that a scaled reproduction of the building motion has been obtained, means that fluctuating aerodynamic forces that depend upon that motion have been reproduced in the wind tunnel. This is not the case when fixed models are used to measure the fluctuating wind pressures, or the 'base balance' technique is used. In both these cases, the resonant response of the building is not reproduced.

Even buildings that have a non-linear mode shape can often be modelled by means of rigid-body rotation, but in these cases it may be appropriate to position the pivot point at a different level to ground level. For example, a building supported on stiff columns near ground level might be modelled by a rigid model pivotted at a height above ground level (e.g. Isyumov *et al.*, 1975). The disadvantage of this approach is that the bending moment at ground level cannot be measured.

There is a direct analogy between the generalised mass of the prototype building, G_1, and the moment of inertia of the model building, including the contributions from the support shaft and any other moving parts.

Assuming that the mode shape of the building is given by:

$$\phi_1 (z) = (z/h) \tag{7.4}$$

the generalised mass is given by:

$$G_1 = \int_0^h m(z)\phi_1^2(z)dz \tag{7.5}$$

The equivalent prototype moment of inertia for rigid body rotation about ground level is then:

$$I_p = \int_0^h m(z)z^2dz = (1/h^2)\ G_1 \tag{7.6}$$

The equivalent model moment of inertia is then given by:

$$I_m = M_r\ L_r^2 I_p = L_r^5(1/h^2)\ G_1 \tag{7.7}$$

where M_r and L_r and are the mass ratio and length ratio, respectively. In order to maintain a density ratio of unity in both model and full scale, assuming that air is the working fluid in both cases,

$$M_r = L_r^3 \tag{7.8}$$

Equation (7.7) can be used to establish the required model moment of inertia.

In order to obtain the correct moment of inertia, and at the same time to achieve a relatively rigid model, it is normally necessary to manufacture the model from a light material such as expanded foam, or balsa wood. A typical mounting is shown in Figure 7.9. The model is supported by gimbals of low friction, and rotation about any horizontal axis is permitted. Elastic support can be provided by springs whose position can be adjusted vertically. In the case of the system shown in Figure 7.9, damping is provided by an eddy current device, but vanes moving in a container of viscous liquid can also be used.

The moment of inertia of the model and the supporting rod and damper plates can be determined in one or more of the following three ways:

- By swinging the model, supporting rod and attachments, as a compound pendulum and measuring the period of oscillation
- By measuring the frequency of vibration in the mounted position, and knowing the spring constants
- By measuring the angular deflection of the supporting rod for known overturning moments applied to the model in position and using the measured frequencies.

The support system shown in Figure 7.9 is the most common arrangement, but a method of support based on a cantilever support has also been used. The vertical position of the model on the cantilever is adjusted to minimise the rotation at ground level. The advantage of this method is that base shear, as well as base bending moment, can be measured.

Testing of the model to determine either the base bending moment or the tip deflection over a range of reduced velocities should be carried out. The assumptions made to justify the rigid model aeroelastic testing, result in a relationship between the base bending moment, M_b, and the tip deflection, x, as follows:

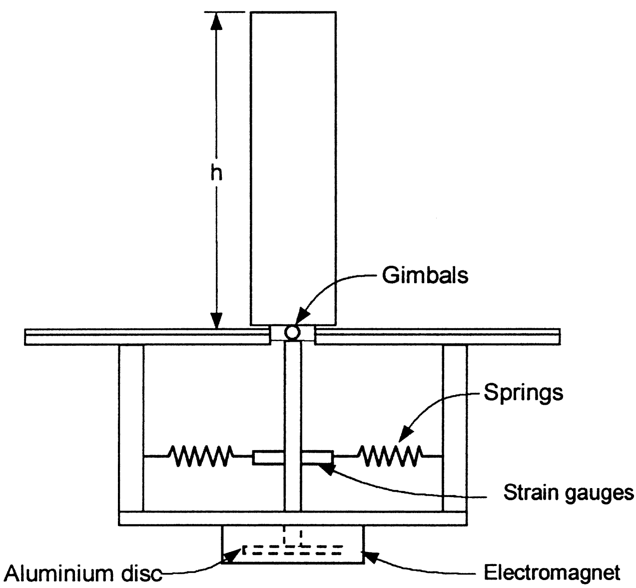

Figure 7.9 A base-pivotted tall building model.

$$M_b = (\omega_1^2 \, I_p/h)\, x = (\omega_1^2 \, G_1/h^3)\, x \cong (\omega_1^2 \, m\, h^2/3)\, x \qquad (7.9)$$

where ω_1 is the natural circular frequency, and m is an average mass/unit height.

The relationship in equation (7.9) implies that the mean and background wind loads are distributed over the height of the building in the same way as the resonant response, i.e. according to the distribution of inertial forces for first mode response. This is a consequence of the neglect of the higher modes of vibration.

The upper limit of reduced velocity should correspond to a mean wind speed which is larger than any design value for any wind direction. As it will be required to fit a relationship between response (either peak or r.m.s.) and mean wind speed, testing should be carried out at least three reduced velocities.

It is wise to conduct aeroelastic tests for at least two different damping ratios – a value representative of that expected at perceptible accelerations for the height and construction type, and a higher value that may be achieved at ultimate conditions, or at serviceability design conditions when an auxiliary system is added. If the resonant response is dominant, values outside these conditions can be estimated by assuming that the r.m.s response varies as the inverse of the square root of the damping ratio.

The final stage of an aeroelastic investigation should be to provide the structural engineer with vertical distributions of loads which are compatible with the base bending moments obtained from the experiments and subsequent processing. As discussed in Chapter 5, there are different distributions for the mean component, background or sub-resonant fluctuating component, and the resonant component of the peak response, for any wind direction. If wind tunnel pressure measurements are available, these can be used to determine the mean load distribution. Pressure measurements could, in principle, also be used to determine the background fluctuating loads, although this requires extensive correlation measurements; also the loading distribution should also be 'tailored' to the particular load effect, such as a column load.

For tall buildings, a linear loading distribution with a maximum at the top, reducing to zero at the pivot point, is often assumed. Then the load per unit height at the top of the building, w_0, is given by:

$$w_0 = 3M_b \,/\, h^2 \qquad (7.10)$$

For a linear mode of vibration, this is a realistic distribution for the inertial loading of the resonant part of the response (Section 5.4.4). However this is not a realistic distribution for the mean (Section 5.4.2) or the background response (Section 5.4.3), when the loading is primarily along-wind.

7.6.2 The base balance technique

A technique that has now replaced aeroelastic model testing for a large number of tall buildings in many wind tunnel laboratories is the so-called 'high-frequency base-balance' technique (Tschanz and Davenport, 1983). In this technique, there is no attempt to model the aeroelastic properties of the building – in fact the support system is made deliberately stiff to put the building model above the range of the exciting forces of the wind. A rigid model, which reproduces the building shape, is used. The model is supported at the base by a measurement system, which is capable of measuring the mean and fluctuating wind forces and moments to a high frequency, without significant amplification or attenuation. The spectral densities of the base forces and moments are measured, and the response of the building, with appropriate dynamic properties incorporated, is computed using a spectral or random vibration approach, similar to that described in Section 5.3 of Chapter 5. A range of damping ratios and mean wind speeds can be simulated using this approach.

Figure 7.10 shows how the spectrum of wind force varies with different speeds in a wind tunnel. For a given design of balance there will be an upper limit to the wind force (proportional to wind speed squared) that is capable of being measured by the balance; this will be proportional to the stiffness of the balance for a particular force component. Thus the maximum wind tunnel speed for which a balance can be used is proportional to the square root of the stiffness. Since the natural frequency of a model of given mass is also proportional to the square root of the stiffness, the ratio of maximum wind speed to maximum usable frequency will be a constant for a given design of balance.

When the prototype building does not have a linear sway mode shape, corrections are required to the computed response, as they are for the the base-pivotted aeroelastic model technique. Base torque can also be measured and used to determine the response in torsional mode of vibration, although quite large mode shape corrections are required as the base torque corresponds to a modal force with a uniform mode shape.

The base-balance technique clearly reduces the amount of wind tunnel testing time by a large factor, at the expense of computing resources, which have rapidly become cheaper. However, in those cases where motion-induced, or aeroelastic, forces (Section 5.5) are significant, it is necessary to continue to use aeroelastic modelling to determine wind-induced dynamic response. Most tall buildings, however, can adequately be studied using the base-balance technique – a very cost-effective method.

7.6.3 Sectional and taut strip models of bridges

A common, and long-standing, technique to confirm the aerodynamic stability of the decks of long-span suspension or cable-stayed bridges is the section model test. This is another form of rigid body aeroelastic modelling. The technique dates back to the investigations following the failure of the first Tacoma Narrows bridge (Farquarson *et al.*, 1949–54). A short section of the bridge deck is supported on springs and allowed to move in translation and rotation. By suitable adjustment of the springs, the model frequencies in rotation and vertical translation can be arranged to have the same ratio as those for the primary bending and torsional modes of the prototype bridge. Then in order to achieve similarity between model, *m*, and prototype, *p*, the reduced frequencies (Section 7.4) should be kept equal:

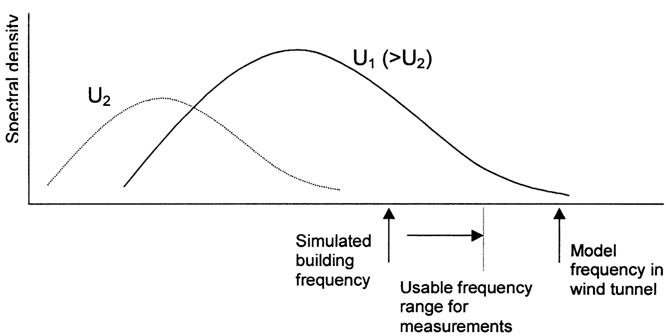

Figure 7.10 Frequency relationships for a high-frequency base balance.

$$\left(\frac{n_s L}{U}\right)_m = \left(\frac{n_s L}{U}\right)_p \qquad (7.11)$$

where n_s should be taken both as the lowest frequencies in vertical translation (bending), and in rotation (torsion).

The models are made as rigid as possible, but they are also required to satisfy the density scaling requirement that the ratio ρ_s/ρ_a should be the same in model and full scale, where ρ_s is the average density of the structure, and ρ_a is the air density. The details of the deck at the leading edge – such as edge beams and guard railings are usually modelled in some detail, as these have been found to affect the aeroelastic behaviour.

Section models are primarily used to determine the critical flutter speeds of the section in both both smooth and turbulent flow. The static aerodynamic coefficients can also be determined for use in calculations of turbulent buffeting of the section. A more advanced use is for determination of the aeroelastic coefficients, or flutter derivatives (Sections 5.5.3 and 12.3.2), for subsequent use in more complete computational modelling of bridge behaviour; both free- (Scanlan and Tomko, 1971) and forced vibration (e.g. Matsumoto *et al.*, 1992) methods have been developed.

Sectional models are primarily a two-dimensional simulation, and cannot readily be used in turbulent flow, which of course is more representative of atmospheric flow and three-dimensional in nature. A more advanced test method for bridges, known as 'taut strip', involves the central span of the model bridge deck supported on two parallel wires, pulled into an appropriate tension, and separated by an appropriate distance, so that the bending and torsional modes are approximately matched. The deck is made in elements or short sections, so that no stiffness is provided. Such a model can be tested in full simulated boundary-layer flows, but is more economical than a full aeroelastic model test.

Scanlan (1983) and Tanaka (1990) have given useful reviews of the section model and taut-strip techniques for bridge decks, together with a discussion of full aeroelastic model testing of bridges.

7.6.4 Multi-mode aeroelastic modelling

For the modelling of structures with non-linear mode shapes, or for structures which respond dynamically to wind in several of their natural resonant modes of vibration, such as tall towers and long-span bridges, the rigid body modelling technique is not sufficient. In the case of long-span bridges, the aerodynamic influences of the cables and the supporting towers, which are not included in section model or taut-strip testing (Section 7.6.3), may often be significant. More complete aeroelastic and structural modelling techniques are then required.

There are three different types of these multi-mode models:

- 'Replica' models – in which the construction of the model replicates that of the prototype structure
- 'Spine' models which reproduce the stiffness properties of the prototype structure by means of smaller central members or 'spines'. Added sections reproduce the mass and aerodynamic shape of the prototype
- 'Lumped mass' models, in which the mass of the model is divided into discrete 'lumps', connected together by flexible elements. The number of vibration modes that can be reproduced by this type of model is limited by the number of lumped masses

The design of these models generally follows the scaling laws based on dimensional analysis, as outlined in Section 7.2. Full model testing of suspension bridges and cable suspended roofs, where stiffness is, at least partially, provided by gravitational forces, requires equality of Froude number, $U/\sqrt{(Lg)}$, (introduced in Section 7.4), between model and full scale. Thus:

$$\left(\frac{U}{\sqrt{Lg}}\right)_m = \left(\frac{U}{\sqrt{Lg}}\right)_p$$

since the gravitational constant, g, is the same in model and full scale, this results in a velocity scaling given by:

$$\frac{U_m}{U_p} = \sqrt{\frac{L_m}{L_p}} \tag{7.12}$$

Thus the velocity ratio is fixed at the square root of the length ratio (or model scale). Thus for a 1/100 scale suspension bridge model, the velocity in the wind tunnel is one tenth of the equivalent velocity in full scale.

For the majority of structures, in which the stiffness is provided by internal stresses (e.g. axial, bending, shear), Froude number scaling is not required for aeroelastic models, and a free choice can be made of the velocity scaling when designing a model. Usually a fine adjustment of the velocity scaling is made after the model is built, to ensure equality of reduced frequency (see equation 7.11).

Examples of aeroelastic models are shown in Figures 11.6 (observation tower) and 12.7 (bridge under construction). These are both 'spine' models.

A further simplification of dynamic models, which is occasionally employed, is to distort, by equal factors, the stiffness and mass properties of the model from those required by the correct scaling laws. This retains the correct value of reduced frequency (Section 7.4) and preserves the correct relationship between the frequencies associated with the flow (e.g. turbulence and vortex shedding), and those related to the structure. Although internal forces and moments in the structure are correctly modelled, deflections, velocities and accelerations of the model, and hence motion-induced forces, such as aerodynamic damping (Section 5.5.1) are not scaled correctly. This type of simplification is used to reduce the cost of model making, when aeroelastic effects are not regarded as important.

7.6.5 Aeroelastic modelling of chimneys

Chimneys and other slender structures of circular cross-sections are vulnerable to cross-wind excitation by fluctuating pressures due to vortex-shedding (Sections 4.6.3 and 11.5). In the 1950s and 1960s, it was quite common to investigate this behaviour with small-scale wind tunnel models. However the forces from vortex shedding are quite dependent on Reynolds number (Section 4.2.4), and wind tunnel tests will severely over-estimate the cross-wind response of prototype large chimneys (Vickery and Daly, 1984). The prediction of full-scale response of such structures is better undertaken by the use of mathematical models of the response (Section 11.5) with input parameters derived from full-scale measurements at high Reynolds numbers.

7.6.6 Structural loads through pressure measurements

For structures such as large roofs of sports stadiums, or large low-rise buildings, with structural systems that are well-defined and for which resonant dynamic action is not dominant, or can be neglected, wind tunnel pressure measurements on rigid models can be used effectively to determine load effects such as member forces and bending moments, or deflections. This method is normally used in conjunction with the area-averaging pressure technique described in Section 7.5.2. Also required are *influence coefficients,* representing the values of a load effect under the action of a single uniformly distributed static 'patch load' acting on the area corresponding to a panel on the wind tunnel model. Two methods are possible.

- Direct on-line weighting of the fluctuating panel pressures recorded in the wind tunnel test with the structural influence coefficients, to determine directly fluctuating and peak values of the load effects (Surry and Stathopoulos, 1977).
- Measurement of correlation coefficients between the fluctuating pressures on pairs of panels, and calculation of root-mean-square and peak load effects by integration, (Holmes and Best, 1981; Holmes *et al.*, 1997).

The latter method has advantages that the influence coefficients are not required at the time of the wind tunnel testing, and also that the information can be used to determine equivalent static load distributions, as discussed in Chapter 5. When resonant response is of significance, as may be the case for the largest stadium roofs, time histories of the fluctuating pressures can be used to generate a time history of generalised force for each mode of significance. From the spectral density of the generalised force, the mean square generalised displacement (modal coordinate), and effective inertial forces acting can be determined (Section 5.4.4). The application of pressure model studies to large roofs is discussed in Chapter 10.

Pressure-based methods can also be used for structural loads and response of tall buildings (A.S.C.E., 1999). Although these methods require a large number of simultaneous pressure measurements and extensive post-processing of the wind tunnel data, accurate account of non-linear resonant mode shapes can be made.

7.7 Blockage effects and corrections

In a wind tunnel with a closed test section, the walls and roof of the wind tunnel provide a constraint on the flow around a model building or group of buildings, which depends on the blockage ratio. The blockage ratio is the maximum cross-sectional area of the model at any cross-section, divided by the area of the wind tunnel cross-section. If this ratio is high enough, there may be significant increases in the flow velocities around, and pressures on, the model. In the case of an open test section, the errors are in the opposite direction; that is the velocities around the model are reduced. To deal with the blockage problem, several approaches are possible:

- Ensure that the blockage ratio is small enough that the errors introduced are small, and no corrections are required. The usual rule for this approach is that the blockage ratio should not exceed 5%.
- Accept a higher blockage ratio, and attempt to make corrections. The difficulty with this approach is that the appropriate correction factors may themselves be uncertain.

Although, there are well documented correction methods for drag and base pressure on stalled airfoils, and other bluff bodies in the centre of a wind tunnel with uniform, or homogeneous turbulent flow, there is very little information for buildings or other structures, mounted on the floor of a wind tunnel in turbulent boundary-layer flow. McKeon and Melbourne (1971) provided corrections for *mean* windward and leeward pressures, and total drag force, on simple plates and blocks. However, no corrections are available for pressures, mean or fluctuating, in separated flow regions, such as occur on roofs or side walls of building models.

- Design the walls and/or roof of the working section in such a way as to minimise the blockage errors. The most promising method for doing this appears to be the *slotted wall* concept (Parkinson, 1984; Parkinson and Cook, 1992). In this system, the walls and roof of the test section are composed of symmetrical aerofoil slats, backed with a plenum chamber. The optimum open area ratio is about 0.55, and it is claimed that blockage area ratios of up to 30% can be used without correction.

7.8 Computational wind engineering

Computational fluid dynamics (CFD) techniques as applied to wind engineering, have been under development for a number of years. There have been several conferences on the subject. It is clear that wind flow around buildings is a very complex fluid mechanics problems, involving a large range of turbulence scales – varying from the very large eddy structures of atmospheric turbulence (see Chapter 3) to the small scales generated by the flow around the bluff-body shapes of buildings and other structures (Chapter 4). The result of this is that, at the time of writing, the most common CFD techniques are capable of predicting the *mean* pressures on buildings with reasonable accuracy, but are not sufficiently accurate for the fluctuating and peak pressures. As an example, mean pressures on arched-roof buildings generated by CFD are discussed in Section 10.3.

The poor representation of the pressure fluctuations is primarily because it is necessary to incorporate over-simplified representations of the turbulence in the fluid flow equations. At the current rate of progress, this situation is unlikely to change for at least the first decade of the twenty-first century.

CFD techniqes are, however, capable currently of providing useful insights into wind flow around buildings for environmental considerations. Useful reviews of such techniques are given by Baskaran and Kashev (1996) and Stathopoulos and Baskaran (1996).

7.9 Summary

In this chapter, a review of methods of laboratory simulation of natural strong wind characteristics for the investigation of wind pressures, forces and structural response has been given. Early methods used natural growth of boundary layers on the floor of wind tunnels to simulate the mean flow and turbulence structure in the fully-developed boundary layer in gale wind conditions. To make use of shorter test sections in aeronautical wind tunnels, rapid growth methods were developed, and were described. For investigations on smaller structures, such as low-rise buildings, methods of simulating only the lower part, or surface layer, of the atmospheric boundary layer were devised.

Methods of simulating strong winds in tropical cyclones and thunderstorms, which are the dominant types for structural design at locations in the tropics and subtropics at latitudes from 0 to 40 degrees, are still at an early stage of development. A major problem is the lack of good full-scale data of the wind structure, on which the simulations can be based.

Experimental methods of measuring local pressures, and overall structural loads in wind tunnel tests are described in Sections 7.5 and 7.6, and the problem of wind tunnel blockage, and its correction is discussed in Section 7.7.

References

American Society of Civil Engineers (1999) 'Wind tunnel studies of buildings and structures', ASCE Manual and Reports on Engineering Practice No. 67. A.S.C.E., New York.

Australasian Wind Engineering Society (2001) 'Wind-engineering studies of buildings', Quality Assurance Manual. AWES-QAM-1-2001.

Aynsley, R. D., Melbourne, W. H. and Vickery, B. J. (1977) *Architectural Aerodynamics*, London: Applied Science Publishers.

Baskaran, A. and Kashev, A. (1996) 'Investigation of air flow around buildings using computational fluid dynamics techniques', *Engineering Structures* 18: 861–75.

Bergh, H. and Tijdeman, H. (1965) 'Theoretical and experimental results for the dynamic response of pressure measurement systems', National Aero- and Astronautical Research Institute (Netherlands), Report NLR-TR-F.238, January 1965.

Cermak, J. E. (1971) 'Laboratory simulation of the atmospheric boundary layer', *AIAA Journal* 9: 1746–54.

—— (1977) 'Wind-tunnel testing of structures', *ASCE Journal of the Engineering Mechanics Division* 103: 1125–40.

Counihan, J. (1969) 'An improved method of simulation of an atmospheric boundary layer in a wind tunnel', *Atmospheric Environment* 3: 197–214.

Cook, N. J. (1973) 'On simulating the lower third of the urban adiabatic boundary layer in a wind tunnel', *Atmospheric Environment* 7: 691–705.

Davenport, A. G., and Isyumov, N. (1967) 'The application of the boundary layer wind tunnel to the prediction of wind loading', *Proceedings, International Research Seminar on Wind Effects on Buildings and Structures*, Ottawa, Canada, 11–15 September, 201–30.

Durgin, F. (1982) 'Instrumentation requirements for measuring aerodynamic pressures and forces on buildings and structures', in T. Reinhold (ed.), *Wind Tunnel Modeling for Civil Engineering Applications*, Cambridge University Press.

Farquarson, F. B., Smith, F. C. and Vincent, G. S. (1949–54) 'Aerodynamic stability of suspension bridges with special reference to the Tacoma Narrows Bridge', *University of Washington Engineering Experiment Station. Bulletin No. 116*, Parts I to V.

Flachsbart, O. (1932) 'Winddruck auf geschlossene und offene Gebäude', in L. Prandl and A. Betz (eds) *Ergebnisse der Aerodynamischen Versuchanstalt zu Göttingen, IV. Lieferung*. Munich and Berlin: Verlag von R. Oldenbourg.

Gerstoft, P. and Hansen, S. O. (1987) 'A new tubing system for the measurement of fluctuating pressures', *Journal of Wind Engineering and Industrial Aerodynamics* 25: 335–54.

Gumley, S. J. (1981) Tubing systems for the measurement of fluctuating pressures in wind engineering', D.Phil. Thesis, University of Oxford.

—— (1983) 'Tubing systems for pneumatic averaging of fluctuating pressures', *Journal of Wind Engineering and Industrial Aerodynamics* 12: 189–228.

—— (1984) 'A parametric study of extreme pressures for the static design of canopy structures', *Journal of Wind Engineering and Industrial Aerodynamics* 16: 43–56.

Holmes, J. D. (1984) 'Effect of frequency response on peak pressure measurements', *Journal of Wind Engineering and Industrial Aerodynamics* 17: 1–9.

—— (1987) 'Distribution of peak wind loads on a low-rise building', *Journal of Wind Engineering and Industrial Aerodynamics* 29: 59–67.

—— (1995) 'Methods of fluctuating pressure measurement in wind engineering', in *A State of the Art in Wind Engineering,* Wiley Eastern Limited.

—— (1997) ‘Equivalent time averaging in wind engineering’, *Journal of Wind Engineering and Industrial Aerodynamics* 72: 411–19.

Holmes, J. D. and Best, R. J. (1981) ‘An approach to the determination of wind load effects for low-rise buildings’, *Journal of Wind Engineering and Industrial Aerodynamics* 7: 273–87.

Holmes, J. D., Denoon, R. O., Kwok, K. C. S. and Glanville, M. J. (1997) ‘Wind loading and response of large stadium roofs’, *International Symposium on Shell and Spatial Structures*, Singapore, 10–14 November.

Holmes, J.D. and Lewis, R.E. (1987a) ‘Optimization of dynamic-pressure-measurement systems. I. Single point measurements’, *Journal of Wind Engineering and Industrial Aerodynamics* 25: 249–73.

—— (1987b) ‘Optimization of dynamic-pressure-measurement systems. II. Parallel tube-manifold systems’, *Journal of Wind Engineering and Industrial Aerodynamics* 25: 275–90.

—— (1989) ‘A re-examination of the leaked-tube dynamic pressure measurement system’, *10th Australasian Fluid Mechanics Conference*, University of Melbourne, 5.39–5.42, December.

Holmes, J. D. and Osonphasop, C. (1983) ‘Flow behind two-dimensional barriers on a roughened ground plane, and applications for atmospheric boundary-layer modelling’, *Proceedings, 8th Australasian Fluid Mechanics Conference*, Newcastle, N.S.W.

Holmes, J. D. and Rains, G. J. (1981) ‘Wind Loads on flat and curved roof low rise buildings’, Colloque “Construire avec le Vent”, Nantes, France, July 1981.

Irminger, J. O. V. (1894) ‘Nogle forsog over trykforholdene paa planer og legemer paavirkede af luftstrominger’, *Ingenioren* 17.

Irwin, H. P. A. H., Cooper, K. R. and Girard, R. (1979) ‘Correction of distortion effects caused by tubing systems in measurements of fluctuating pressures’, *Journal of Industrial Aerodynamics* 5: 93–107.

Irwin, P. A. (1988) ‘Pressure model techniques for cladding wind loads’, *Journal of Wind Engineering and Industrial Aerodynamics* 29: 69–78.

Isyumov, N., Holmes, J. D., Surry, D. and Davenport, A.G. (1975) ‘A study of wind effects for the First National City Corporation Project, New York’, University of Western Ontario, Boundary Layer Wind Tunnel Special Study Report, BLWT-SS1-75.

Jensen, M. (1958) ‘The model law for phenomena in the natural wind’, *Ingenioren* (International edition) 2: 121–8.

—— (1965). ‘Model scale tests in the natural wind. (Parts I and II)’, Danish Technical Press.

Kareem, A. Cheng, C-M. and Lu, P. C. (1989) ‘Pressure and force fluctuations on isolated circular cylinders of finite height in boundary layer flows’, *Journal of Fluids and Structures* 3: 481–508.

Kernot, W. C. (1893) ‘Wind pressure’, *Proceedings, Australasian Society for the Advancement of Science* V: 573–81.

Larose, G. L. and Franck, N. (1997) ‘Early wind engineering experiments in Denmark’, *Journal of Wind Engineering and Industrial Aerodynamics* 72: 493–9.

Lawson, T. V. (1976) ‘The design of cladding’, *Building and Environment* 11: 37–8.

Matsumoto, M., Shirato, H. and Hirai S. (1992) ‘Torsional flutter mechanism of 2-d H-shaped cylinders and effect of flow turbulence’, *Journal of Wind Engineering and Industrial Aerodynamics* 41: 687–98.

McKeon, R. and Melbourne, W. H. (1971) ‘Wind-tunnel blockage effects and drag on bluff bodies in rough walll turbulent boundary layers’, *Third International Conference on Wind Effects on Buildings and Structures*, Saikon Shuppan Publishers: Tokyo.

Parkinson, G. V. (1984) ‘A tolerant wind tunnel for industrial aerodynamics’, *Journal of Wind Engineering and Industrial Aerodynamics* 16: 293–300.

Parkinson, G. V. and Cook, N. J. (1992) ‘Blockage tolerance of a boundary-layer wind tunnel’, *Journal of Wind Engineering and Industrial Aerodynamics* 42: 873–84.

Reinhold, T. (ed.) (1982) Wind tunnel modeling for civil engineering applications. *International Workshop on Wind Tunnel Modeling Criteria and Techniques in Civil Engineering Applications*, Gaithersburg, Maryland, U.S.A.: Cambridge University Press.

Scanlan, R. H. and Tomko, J. J. (1971) ‘Airfoil and bridge deck flutter derivatives’, *Journal of the Engineering Mechanics Division, ASCE* 97: 1717–37.

Scanlan, R. H. (1983) 'Aeroelastic simulation of bridges', *Journal of Structural Engineering, ASCE* 109: 2829–37.

Stathopoulos, T. and Baskaran, B. A (1996) 'Computer simulation of wind environmental conditions around buildings', *Engineering Structures* 18: 876–85.

Surry, D. and Isyumov, N. (1975) 'Model studies of wind effects – a perspective on the problems of experimental technique and instrumentation', *6th International Congress on Aerospace Instrumentation*, Ottawa.

Surry, D. and Stathopoulos, T. (1977) 'An experimental approach to the economical measurement of spatially-averaged wind loads', *Journal of Industrial Aerodynamics* 2: 385–97.

Tanaka, H. (1990). 'Similitude and modelling in wind tunnel testing of bridges', *Journal of Wind Engineering and Industrial Aerodynamics* 33: 283–300.

Tschanz, T. and Davenport, A. G. (1983) 'The base balance technique for the determination of dynamic wind loads', *Journal of Wind Engineering and Industrial Aerodynamics* 13: 429–39.

Vickery, B. J. and Daly, A. (1984) 'Wind tunnel modelling as a means of predicting the response to vortex shedding', *Engineering Structures* 6: 363–8.

Whitbread, R. E. (1963) 'Model simulation of wind effects on structures', *Proceedings, International Conference on Wind Effects on Buildings and Structures*, Teddington U.K. 26–28 June, 284–302.